

ORIGINAL ARTICLE

Open Access



# Research on the Pressure Regulator Effect on a Pneumatic Vibration Isolation System

Yan Shi<sup>1</sup>, Shaofeng Xu<sup>1,2</sup>, Zhibo Sun<sup>3\*</sup>, Yulong Nie<sup>1</sup> and Yixuan Wang<sup>3\*</sup>

## Abstract

The pneumatic vibration isolator (PVI) plays an increasingly important role in precision manufacturing. In this paper, aiming to detect the performance of the pressure regulator in the PVI system, a PVI testing system with a pressure regulator is designed and developed. Firstly, the structure of the pneumatic spring is presented and analyzed, and the nonlinear stiffness is obtained based on the ideal gas model and material mechanics. Then, according to the working principle and continuity equations of ideal airflow, a dynamic model of the PVI system with a pressure regulator is established. Through the simulation analysis, the vibration isolation performance is improved with the efficient and precise pressure regulator. The average values of both the vibration velocity and transmission rate decrease when the vibration is set to 4, 10, 20 and 40 Hz, respectively. The experiments demonstrate the reliability and effectiveness of the pressure regulator. This achievement will become an important basis for future research concerning precision manufacturing.

**Keywords:** Pneumatic vibration isolators, Pressure regulator, Transmission rate, Rubber stiffness

## 1 Introduction

In recent years, vibration isolation technology plays an increasingly important role in precision manufacturing [1, 2], precision instruments [3, 4] and automatic suspension [5–7]. Compared to other vibration isolation devices, the pneumatic vibration isolator (PVI) has the advantages of low natural frequency [8], variable stiffness rate [9], long life and high energy storage [10, 11]. For the precision industry, especially optical equipment [12], the pneumatic vibration isolation platform system is usually supported by several PVI to attenuate vibration transmitted from the vibration source to the platform. The passive PVI is a simple method for high frequency vibration isolation. The stiffness could be changed with the payload, and the PVI model is widely analyzed, such as the Nishimura model [13], Simpack-based model [14], Vampire-based model [15], and the Berg model [16, 17].

The passive PVI usually maintains high vibration isolation performance for vibration disturbances above 10 Hz, but below 10 Hz vibration isolation performance will decrease and resonance will occur near the system's natural frequency [18]. Active PVI keeps the system stable by using precision servo valves to control the gas in and out of the air spring [19–22]. However, these precision pneumatic servo systems are usually very expensive. In addition, many vibration isolation platforms operate at frequencies greater than the system's natural frequency. Therefore, to reduce costs, the stabilizing effect of the pressure regulator on vibration-induced pressure changes in the air spring cavity is considered in low-frequency vibration control. The pneumatic pressure regulator takes compressed gas as the working medium to convert the high pressure at the inlet into the low pressure at the outlet and maintains the stability of the outlet pressure. The pressure regulating principle is that the air flows through the opening of the valve core to throttle and depressurize. When the upstream input gas pressure fluctuates or the flow of the pressure regulator changes, the function of the pressure regulator is realized by keeping the valve

\*Correspondence: [sunzb@buaa.edu.cn](mailto:sunzb@buaa.edu.cn); [magic\\_wyx@163.com](mailto:magic_wyx@163.com)

<sup>3</sup> Engineering Training Center, Beihang University, Beijing 100191, China  
Full list of author information is available at the end of the article

opening at a certain opening relying on the feedback regulation of the pressure regulator itself. As a basic part, the engineering application level of the pressure regulator is much higher than the level of theoretical research. Hos et al. [23] established a mathematical model of a spring-load pressure relief valve and proved that the simplified models can predict the occurrence of flutter instability in oscillation valves. Prescott et al. [24] built several models to represent the behaviour of pressure regulators, then, the scope and effect of the model are analyzed. Kato et al. [25] designed a high precision, quick response pneumatic pressure regulator which consists of an isothermal chamber, a servo valve, a pressure sensor, a quick response laminar flow sensor (QFS), and a pressure differential sensor. Wang et al. [26] designed an accurate self-tuning pressure regulator for pneumatic-pressure-load systems. The dynamic characteristics of pneumatic proportional regulator in pneumatic loading system were also analyzed [27].

In order to verify the reliability and effectiveness of the pressure regulator, the structure of the pneumatic spring is presented and analyzed, and the nonlinear stiffness is obtained based on the ideal gas model [28, 29], and finite element method [30, 31]. Then, according to the working principle and continuity equations of ideal air flow, a dynamic model of the PVI system with the pressure regulator was established. The simulation under the Simulink environment is applied to analyze the performance of the pressure regulator. The PVI testing system with a pressure regulator is designed and developed to verify the results of the simulation. Finally, a summary of the results and conclusions is presented.

## 2 Pneumatic Vibration Isolation System

### 2.1 Structure Parameters of the Pneumatic Spring

The structure of the pneumatic spring is presented as shown in Figure 1. It is comprised of a fixed bogie, a moving platform, an air chamber, an air inlet and a rubber

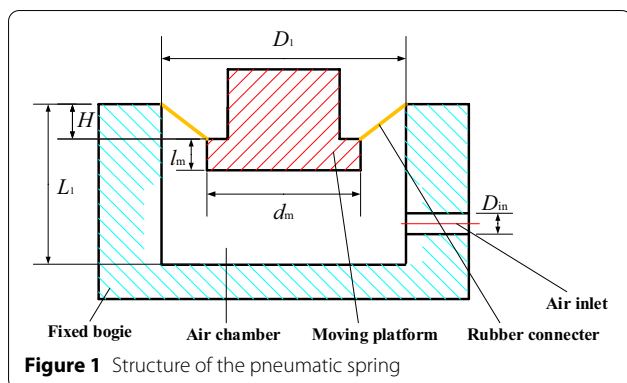


Figure 1 Structure of the pneumatic spring

connector. The fixed bogie is a rigid part connected with the vibration platform by the flange. The moving platform is also a rigid component to support the loads from the isolation platform. The rubber connector connects the moving platform and the fixed bogie, which performs a conical surface. The air chamber is an envelope space surrounded by the fixed bogie, rubber connector and floating platform. The air inlet is a hole in the fixed bogie for air pressure adjustment.

### 2.2 Parameters of the Pneumatic Spring

Vertical stiffness is important for the dynamic characteristic of the pneumatic spring. As can be seen in Figure 1,  $L_1$  is the length of the air chamber,  $D_1$  and  $d_m$  stand for the outer and inner diameters of the rubber connector, and  $l_m$  is the length of the floating displacement inside the air chamber.  $H$  denotes the floating height. The stiffness model is a parallel combination of two parts: the stiffness model of internal compressed air and the stiffness model of the rubber connector. In a sealed container, the ideal gas equation is shown as Eq. (1).

$$P_g V^\lambda = const, \tag{1}$$

where  $\lambda$  is the polytropic coefficient. If the internal temperature is constant, then  $\lambda = 1$ . If part of the gas cannot complete the heat exchange process within a short time or there is not much heat exchange and it is regarded as an adiabatic process, then  $\lambda$  is recorded as 1.4. The volume of the air spring could be divided into two parts: the constant part and the variable part. The constant part could be calculated as:

$$V_{con} = \frac{\pi D_1^2 L_1 - \pi d_m^2 l_m}{4}. \tag{2}$$

As can be seen in Figure 2, the volume of the air chamber changes with the floating height  $H$ . The variable part could be approximately calculated as:

$$V_{var} = \begin{cases} \int_0^H \pi \left( \frac{d_m}{2} + \left( \frac{D_1 - d_m}{2H} \right) h \right)^2 dh & H > 0, \\ - \int_H^0 \pi \left( \frac{d_m}{2} + \left( \frac{D_1 - d_m}{2H} \right) h \right)^2 dh & H \leq 0. \end{cases} \tag{3}$$

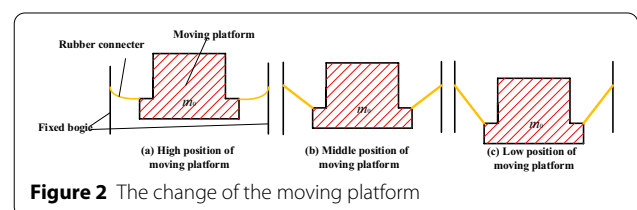


Figure 2 The change of the moving platform

Through the integral, the variable volume could be simplified as:

$$V_{\text{var}} = \frac{\pi H}{12} (D_1^2 + D_1 d_m + d_m^2). \tag{4}$$

The total volume could be calculated as:

$$\begin{aligned} V &= V_{\text{con}} + V_{\text{var}} \\ &= \frac{\pi D_1^2 L_1 - \pi d_m^2 l_m}{4} + \frac{\pi H}{12} (D_1^2 + D_1 d_m + d_m^2). \end{aligned} \tag{5}$$

In order to analyze the relationship of the parameters, new indexes  $\varepsilon_1, \varepsilon_2$  are introduced in the model.  $\varepsilon_1 = d_m/D_1, \varepsilon_2 = l_m/L_1$ . And Eq. (5) could be simplified as:

$$V = \frac{\pi D_1^2}{12} (3L_1(1 - \varepsilon_1^2 \varepsilon_2) + H(1 + \varepsilon_1 + \varepsilon_1^2)). \tag{6}$$

The derivative of the pressure  $P_g$  concerning the height  $H$  could be derived from Eq. (1), and the derivative is obtained as:

$$\frac{\partial P_g}{\partial H} = -\frac{P_g \lambda}{V} \frac{\partial V}{\partial H} = -\frac{\pi D_1^2 \lambda P_g (\varepsilon_1^2 + \varepsilon_1 + 1)}{12V}. \tag{7}$$

The force produced by the pneumatic spring could be described as:

$$F_g = (P_g - P_0) \cdot \frac{\pi}{4} D_1^2, \tag{8}$$

where  $P_0$  is the pressure of the atmosphere. In this pneumatic spring model, the effective area is defined as  $A_{\text{ef}} = \pi D_1^2/4$ . Referring to Eqs. (7) and (8), the stiffness of the air can be expressed as:

$$k_g = \frac{\partial F_g}{\partial H} = \frac{P_g \lambda A_{\text{ef}}^2 (\varepsilon_1^2 + \varepsilon_1 + 1)}{4V}. \tag{9}$$

### 2.3 Parameters Model of the Rubber Connector

The vertical elastic stiffness of the rubber  $k_x$  could be analyzed based on the finite element. In the pneumatic spring structure, rubber shapes a conical surface. It is assumed that the rubber material presents a smooth characteristic. Based on the finite element analysis, the rubber connector could be divided into small elements. As shown in Figure 3, a rubber connector is a composition of the parallel element rubber stick. Each stick could be recognized as a series of rubber pieces. The elastic stiffness of the rubber connector is a series and parallel structure of the rubber pieces.

It is assumed that the rubber material presents a smooth characteristic. Based on the material mechanics, the stiffness of the rubber can be integrated as:

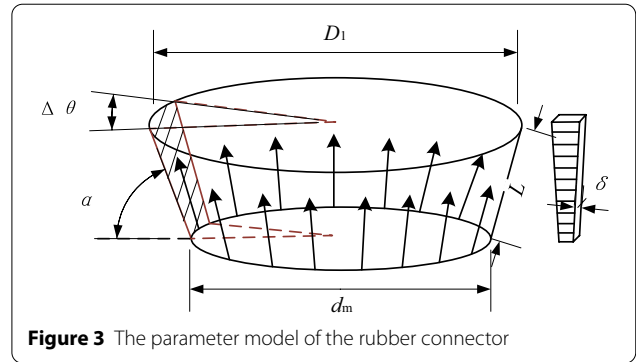


Figure 3 The parameter model of the rubber connector

$$k_x = \int_0^{2\pi} \frac{\sin \alpha}{\int_0^L \frac{dl}{E \cdot dS}} = \int_0^{2\pi} \frac{\sin \alpha}{\int_0^L \frac{dl}{E \cdot \left( \frac{D_1 l - d_m l + d_m L}{L} \right) \delta \cdot \Delta \theta}}, \tag{10}$$

where  $E$  denotes Young's modulus of the rubber,  $L$  means the elongation length of the rubber and  $H = L \sin \alpha, \delta$  is the thickness of the rubber. Through integral, the stiffness of the rubber could be calculated as:

$$k_x = -\frac{E \delta \times \pi \times \left( \frac{1}{\varepsilon_1} - 1 \right) d_m H}{\left( H^2 + \left( \frac{D_1 - d_m}{2} \right)^2 \right) \times \ln \frac{1}{\varepsilon_1}}. \tag{11}$$

It is assumed that  $h_0$  is the activating length of the rubber spring, which is 10 mm. The rubber spring will not work if the parameter  $H$  does not reach  $h_0$ . Thus, the stiffness of the pneumatic spring can be determined from the aforementioned equations as Eq. (12).

$$k = \begin{cases} k_g & H \leq h_0, \\ k_x + k_g & H > h_0. \end{cases} \tag{12}$$

### 2.4 Natural Frequency Analysis of the Testing System

Based on the dynamic analysis, this is the free vibration of the coulomb damping system. Coulomb damping has no effect on the natural frequency of the simple harmonic vibration, the natural frequency would be obtained as:

$$\omega = \frac{1}{2\pi} \sqrt{\frac{k}{m_0}}, \tag{13}$$

where  $k$  is the stiffness of the system, and could be expressed as:

$$k = k_g + k_x. \tag{14}$$

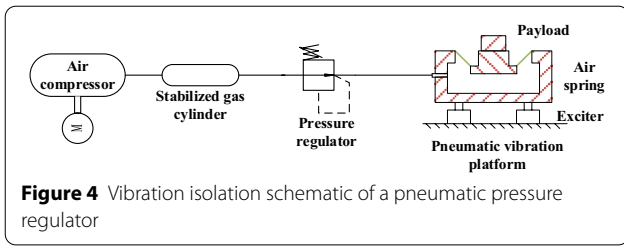


**Figure 4** Vibration isolation schematic of a pneumatic pressure regulator

### 2.5 Vibration Transmission Rate Analysis

The vibration isolation effect of a nonlinear vibration isolation system is evaluated using its transmission rate, which is defined as the ratio of corresponding vibration energy before and after the vibration isolation system [32]. The expression can be presented as:

$$T_d = \sqrt{E[\dot{x}^2]/E[\dot{x}_b^2]}, \tag{15}$$

where  $E[\dot{x}^2]$  and  $E[\dot{x}_b^2]$  denote the mean square of the frame and pavement velocity.

A schematic diagram of the pneumatic vibration isolation using a pressure regulator is shown in Figure 4. The compressor provides enough high-pressure gas, and the stabilized gas cylinder stabilizes the air pressure output by the air compressor to eliminate the effect of motor and environmental changes on the air pressure. Subsequently, the compressed air enters the new air spring through the pressure regulator, relying on the pressure stabilization effect of the pressure regulator to reduce the vibration generated by the exciter and realize the vibration isolation of the load.

## 3 Model of Pressure Regulator

### 3.1 Structure of the Pressure Regulator

As shown in Figure 5, the diaphragm pressure regulator mainly includes the following parts: pressure regulating spring, relief hole, diaphragm, main spool and main spool spring. The working principle of the diaphragm pressure regulator is as shown in Figure 5.

The pressure regulating spring is compressed to push the diaphragm down, and the main spool is open. The inlet pressure  $p_1$  is throttled and depressurized through the orifice. Output pressure  $p_2$  rises and generates an upward thrust on the diaphragm. When this thrust is balanced with the force of the pressure regulating spring, the outlet pressure will stabilize at a certain value. The balance function could be calculated as:

$$F_1 + S_2 p_2 = S_1 p_2 + S_2 p_1 + F_2, \tag{16}$$

where  $F_1$  is the pre-force of the pressure regulating spring,  $F_2$  is the pre-force of the main spool spring,  $S_1$  is

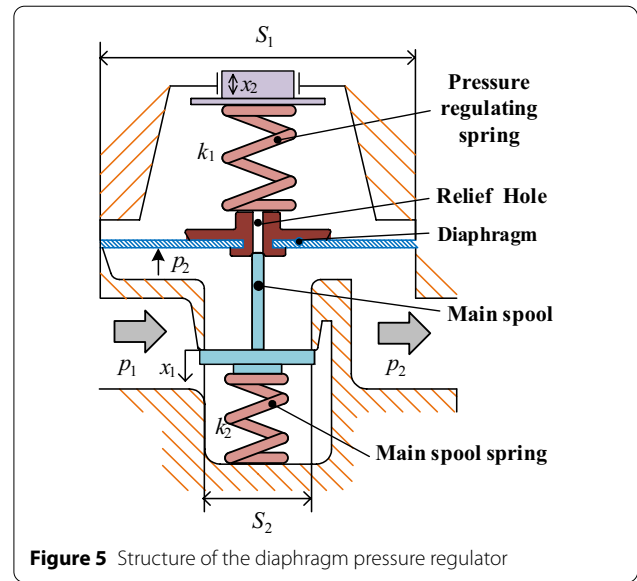


**Figure 5** Structure of the diaphragm pressure regulator

the area of the diaphragm, and  $S_2$  is the area of pressure regulator inlet port.

When setting the pressure (rotary adjustment thread), the main spool opening  $x_1$  is 0, the flow through the pressure regulator is 0, and the outlet pressure can be derived as:

$$p_2 = \frac{F_1 - F_2 - S_2 p_1}{S_1 - S_2}. \tag{17}$$

The pressure rises instantaneously by  $\Delta p_1$ , the outlet pressure also rises, and the thrust acting on the diaphragm increases by  $\Delta p_2$ . The diaphragm moves up and compresses the pressure regulating spring by  $\Delta x$ . If the outlet pressure reaches the set threshold, the overflow will flow through the relief hole in the middle of the diaphragm. The outlet pressure drops back until a new balance reaches. The new balance function could be calculated as:

$$\begin{aligned} F_1 + k_2 \Delta x + S_2(p_2 + \Delta p_2) \\ = S_1(p_2 + \Delta p_2) + S_2(p_1 + \Delta p_1) + F_2 - k_1 \Delta x. \end{aligned} \tag{18}$$

Referring to Eqs. (16) and (17), the increased pressure  $\Delta p_2$  could be calculated as:

$$\Delta p_2 = \frac{(k_2 + k_1) \Delta x - S_2 \Delta p_1}{S_1 - S_2}. \tag{19}$$

### 3.2 Airflow of the Pressure Regulator

The flow of the valve is determined by the inlet pressure  $p_i$  and outlet pressure  $p_o$ . The ratio  $p_o/p_i$  in different cases determines the different airflow equations with

restriction and could be indicated in the continuity equations of ideal airflow:

$$q = \begin{cases} \frac{S_{ep} p_i}{\sqrt{T_i}} \sqrt{\frac{2\kappa}{R(\kappa-1)}} \left[ \left( \frac{p_0}{p_i} \right)^{\frac{2}{\kappa}} - \left( \frac{p_0}{p_i} \right)^{\frac{\kappa+1}{\kappa}} \right] & \frac{p_0}{p_i} > 0.528, \\ \frac{S_{ep} p_i}{\sqrt{T_i}} \left( \frac{2}{\kappa+1} \right)^{\frac{1}{\kappa-1}} \sqrt{\frac{2\kappa}{R(\kappa+1)}} & \frac{p_0}{p_i} \leq 0.528, \end{cases} \quad (20)$$

where  $S_{ep}$  means the effective area of the pneumatic intake and exhaust port,  $\text{mm}^2$ ;  $\kappa$  stands for specific heat ratio; and  $T_i$  means the upstream side temperature, K.

#### 4 Design of the Pneumatic Spring Testing System

##### 4.1 Simulation Analysis of the Vibration Isolation System

The dynamic model of the vibration isolation system with pressure regulator could be established in Figure 6. The main spool opening affects the area of the inlet port. The area of the valve inlet port could be calculated as:

$$s_i = x_1 \cdot \pi d_2. \quad (21)$$

For the relief part,  $S_0$  is the area of the relief port. Based on the dynamic model, the simulation of the testing system is established under Matlab/Simulink environment. The initial parameters of the pneumatic spring are presented in Table 1.

In the simulation, five computing modules are established, which are pressure regulator model, pneumatic spring dynamic model, rubber stiffness model, transmission rate analysis and pressure regulator. The evaluating values such as vibration velocity, pneumatic pressure of the spring and transmission rate are the outputs of the system.

The payload is set as 30 kg, and the amplitude of the vibration is 5 mm. The pressure regulator system and

**Table 1** Initial parameters of the pressure regular

Parameters	Description	Values
$d_2$ (mm)	Diameter of the pressure regular inlet port	6
$d_1$ (mm)	Diameter of the diaphragm	18
$d_0$ (mm)	Diameter of the pressure regular relief port	2
$S_0$ ( $\text{mm}^2$ )	The area of the exhaust port	12.57
$k_1$ (N/mm)	The stiffness of pressure regulating spring	1.5
$k_2$ (N/mm)	The stiffness of main spool spring	12

without pressure regulator system are simulated with the same conditions respectively. From Ref. [33], the ideal air pressure is set as 0.16 MPa. In order to analyze the pressure influence, the setting pressure of the pneumatic and input pressure are respectively set as 0.16 MPa and 0.2 MPa with the pressure regulator. For another system, the initial pressure is set as 0.16 MPa. In the first simulation, the frequency of the signal is set as 4 Hz. The simulation time is 5 s, and the simulation results are shown in Figure 7.

As can be seen in Figure 7, the pressure inside the pneumatic spring shows smooth performance with the pressure regulator. The maximum pressure fluctuation is 0.063 MPa without a valve and 0.023 MPa with the valve respectively. The mean range velocity of the isolation is 0.71 mm/s without a valve and 0.51 mm/s with the valve. The stable transmission rate is 226% without a valve and 191% with the valve respectively.

In the second simulation, the frequency of the signal is set as 10 Hz, shown as Figure 8. The pressure inside the pneumatic spring shows smooth performance with the pressure regulator. The maximum pressure fluctuation is 0.047 MPa without a valve and 0.025 MPa with the valve respectively. The mean range velocity of the isolation is

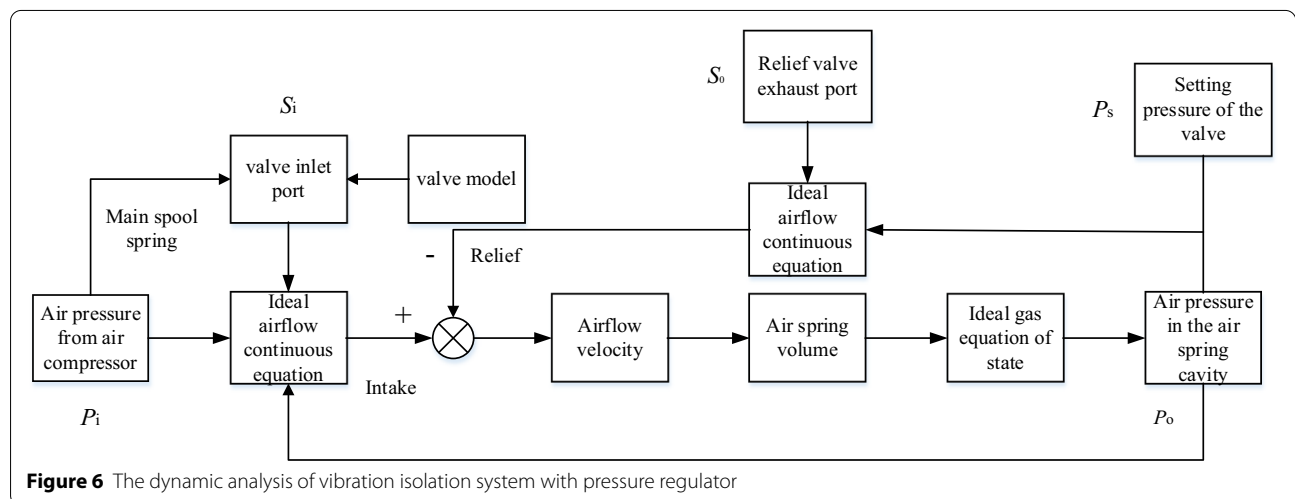
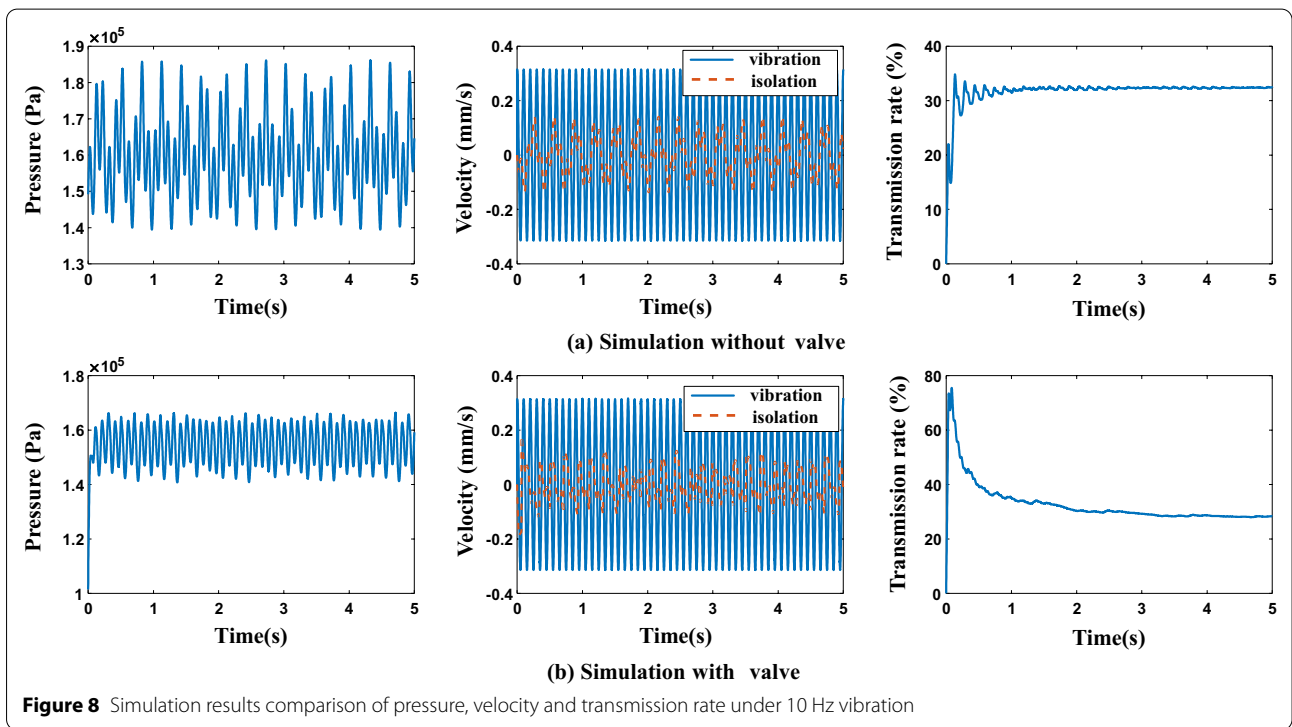
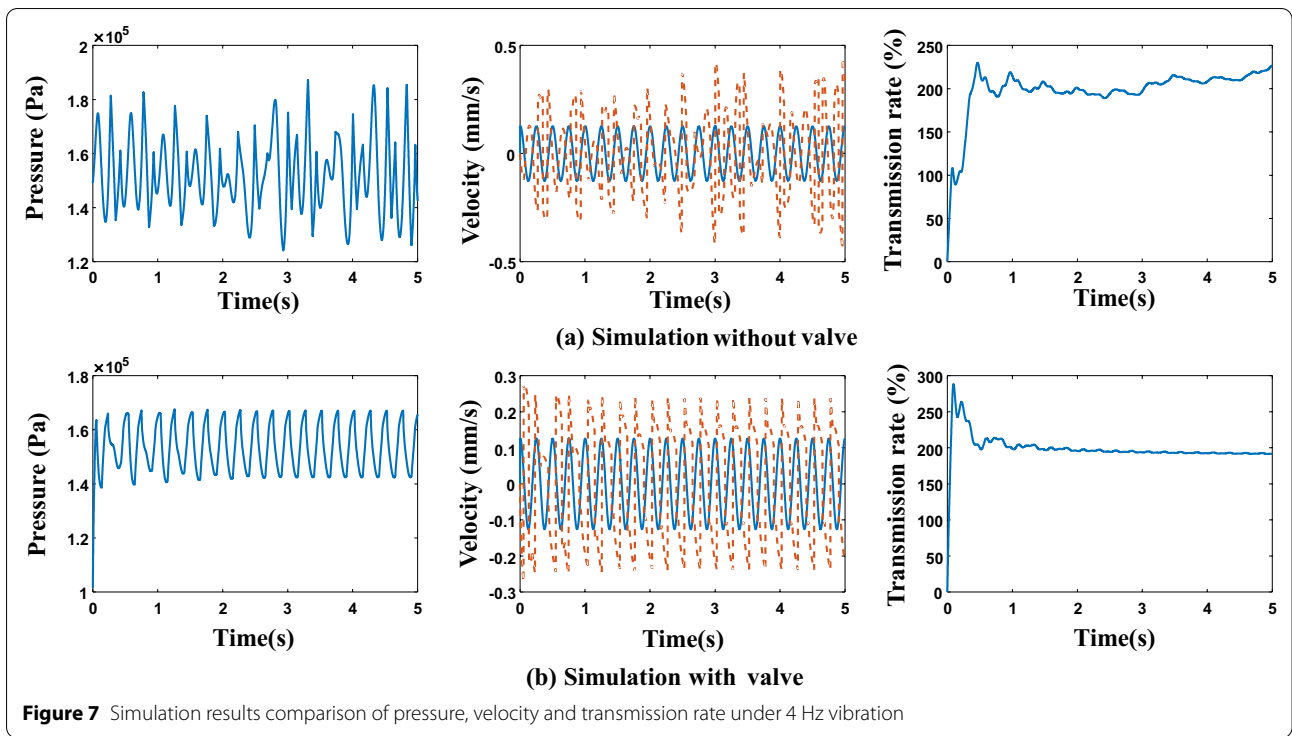
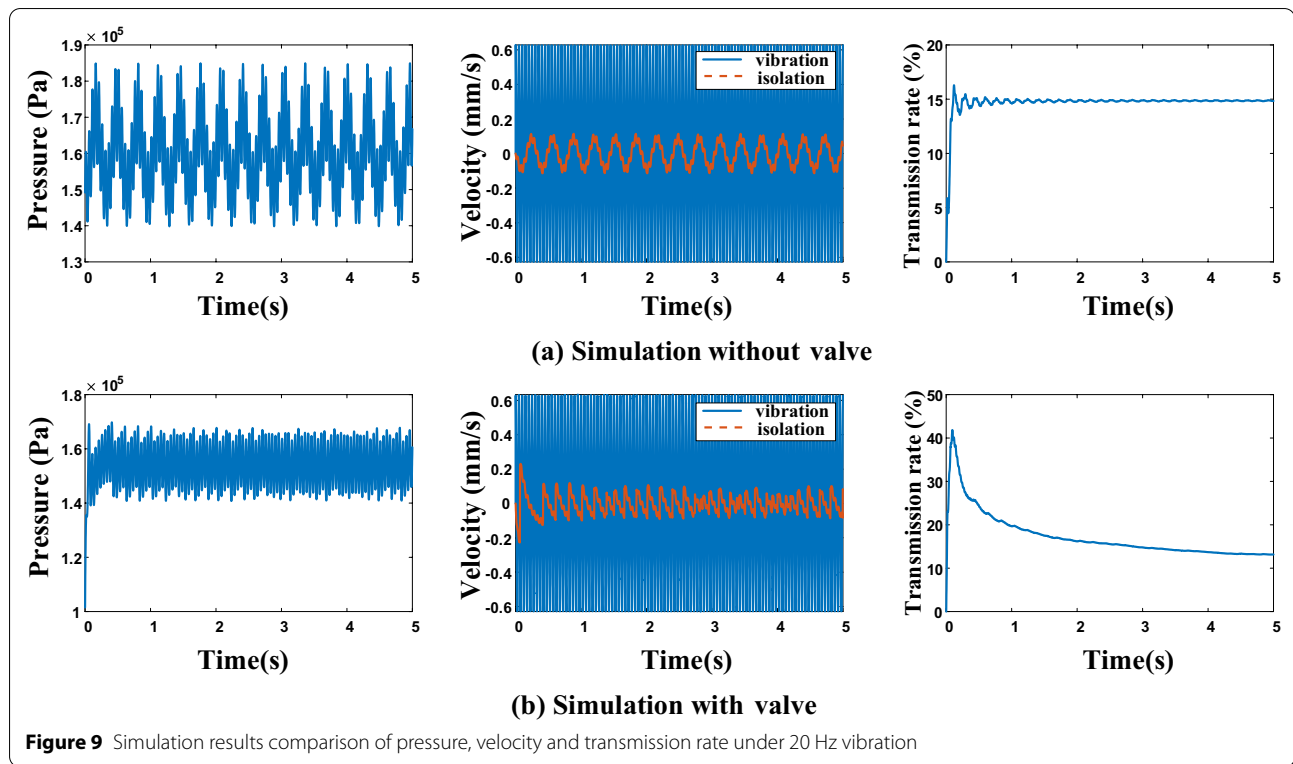


**Figure 6** The dynamic analysis of vibration isolation system with pressure regulator



0.25 mm/s without a valve and 0.20 mm/s with valve. The stable transmission rate is 32.4% without a valve and 28.3% with the valve respectively.

In the third simulation, the frequency of the signal is set as 20 Hz, shown in Figure 9. The pressure inside the pneumatic spring shows smooth performance with the



pressure regulator. The maximum pressure fluctuation is 0.044 MPa without valve and 0.025 MPa with the valve respectively. The mean range velocity of the isolation is 0.21 mm/s without valve and 0.18 mm/s with valve. The stable transmission rate is 14.9% without a valve and 13.2% with the valve respectively.

In the fourth simulation, the frequency of the signal is set as 40 Hz, shown as Figure 10. The pressure inside the pneumatic spring shows smooth performance with the pressure regulator. The maximum pressure fluctuation are 0.044 MPa without valve and 0.025 MPa with the valve respectively. The mean range velocity of the isolation are 0.19 mm/s without valve and 0.16 mm/s with valve. The stable transmission rate are 7.9% without valve and 5.2% with the valve respectively.

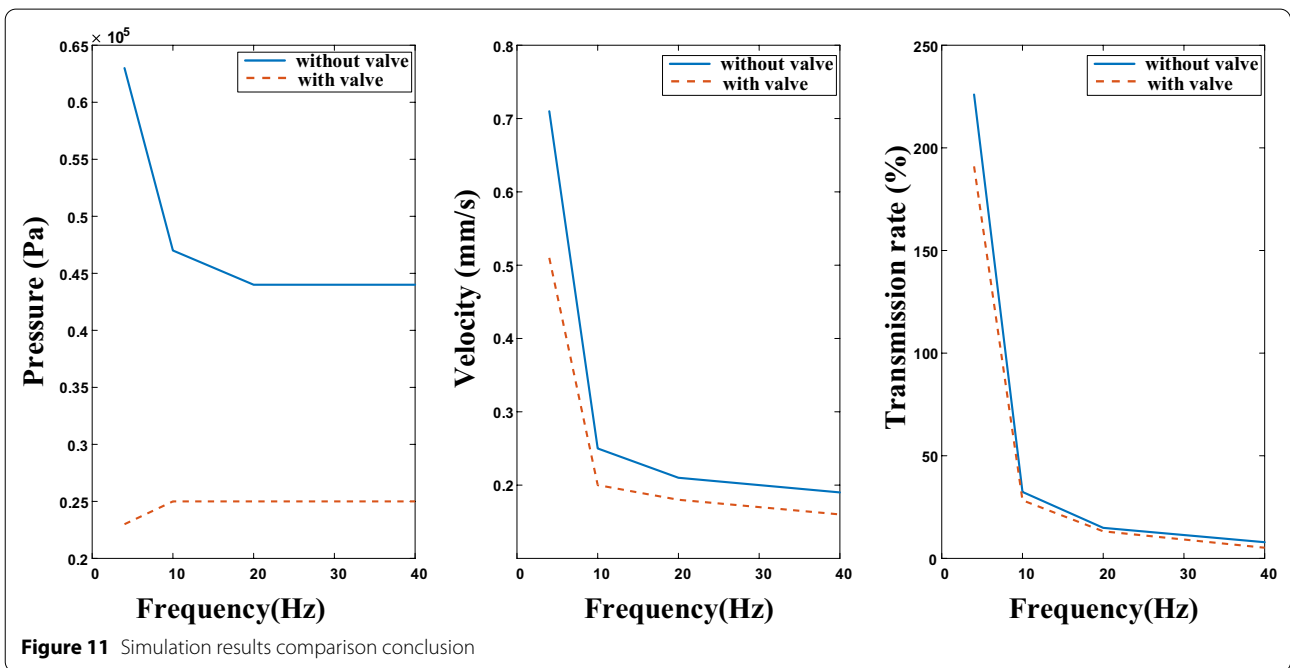
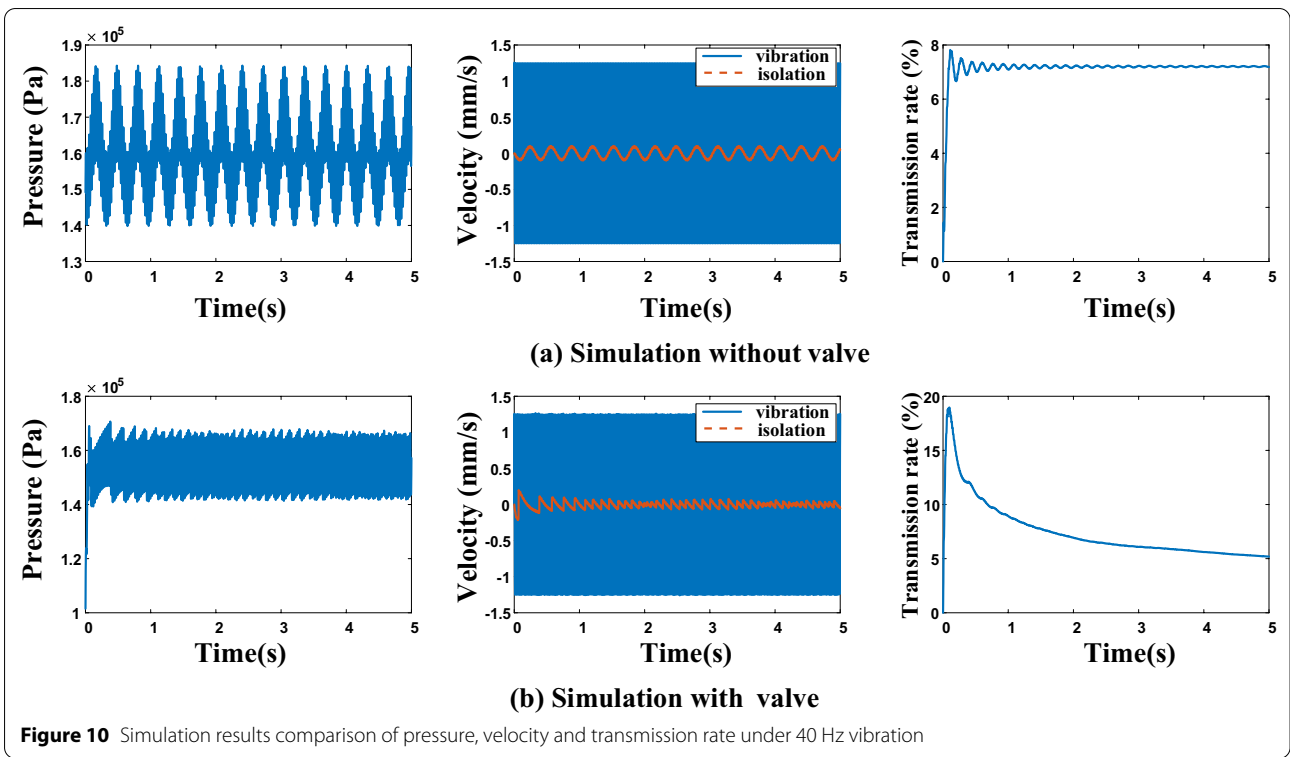
From the simulations above, as can be seen in Figure 11, the following conclusions can be drawn. ① The pressure regulator can improve the stability of air pressure and reduce the vibration velocity and transmission rate in the spring chamber with 4, 10, 20 and 40 Hz vibration frequency. ② The pressure regulator performs better in low frequency vibration. ③ The pressure regulator in the system could not isolate the low frequency vibration such as 4 Hz vibration. Based on the natural frequency analysis, the natural frequency of the experimental system is around 4 Hz, and the vibration is amplified by the vibration isolation system.

## 5 Comparison Between Simulation and Experiment of the Testing System

### 5.1 Scheme of the Experiment System

The pneumatic vibration isolation testing system is shown in Figure 12. Payload stands for the effective mass above the platform, and pressure regulator is a control component of the vibration isolation system. An accelerometer is applied to measure the data of the source and vibration isolation platform. As the main vibration damping element, the gas spring acts between the vibration source and the table. Exciters are used to simulate random vibration sources in the environment. A fixed frame is used to support vibration and isolation platform. Two linear bearings ensure that the transitive vibration direction is vertical. The vibration platform and isolation platform are detected to prove the performance of the pneumatic spring. Besides, air compressors and regulator bottles, as well as some pneumatic ducts, are used to provide air with stable pressure and transmission pressure.

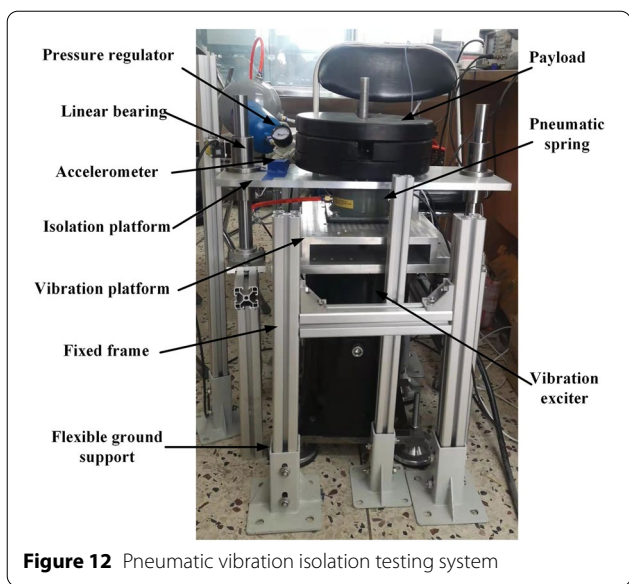
The testing system could realize the parameter detection of under multi-band frequency. The air pressure of the spring and the frequency of the stimulated vibration are variable. The system could test the performance of the springs under different conditions.



### 5.2 Result and Discussion

The payload ranges from 10 to 50 kg with step size 10 in the pneumatic vibration isolation testing system. From Ref. [34], 10 and 50 kg payloads are analyzed, and 30 kg

performs the most stable under the vibration from 20 to 100 Hz. In the experiment, the payload is set as 30 kg, and the vibration frequency is set as 4, 10, 20 and 40 Hz respectively. The condition of the experiment fits that



of the simulation. Based on the integral of the acceleration, the velocity comparison is presented as Figure 13. The transmission rate comparison is shown in Figure 14. With the pressure regulator, the stable transmission rates are 331.1%, 43.3%, 3.6% and 2.9% under 4, 10, 20 and 40 Hz respectively. Compared with the simulation result, the results of the experiment are as follows.

- (1) From the transmission rate results under 4, 10, 20 and 40 Hz, the pneumatic spring proves to be effective under the high vibration frequency. For low-frequency vibration such as 4 Hz, this pneumatic spring loses effectiveness. The experimental results agree with the simulation results.
- (2) Compared with the simulation results, the experiment results show more efficient under the high frequency vibration, and less efficient under the low frequency vibration. The reason might due to the damping of the linear bearing.
- (3) Adding a pressure regulator, the high-frequency vibration is slightly better than the passive effect. But if the pressure of the pressure regulator is not adjusted properly, it will have the opposite effect.

## 6 Conclusions

- (1) A pneumatic spring with a conical rubber connector is presented. The stiffness of the pneumatic spring is analyzed based on the ideal gas model and finite element method. According to the working principle and continuity equations of ideal airflow, a dynamic model of the PVI system with pressure regulator is established.

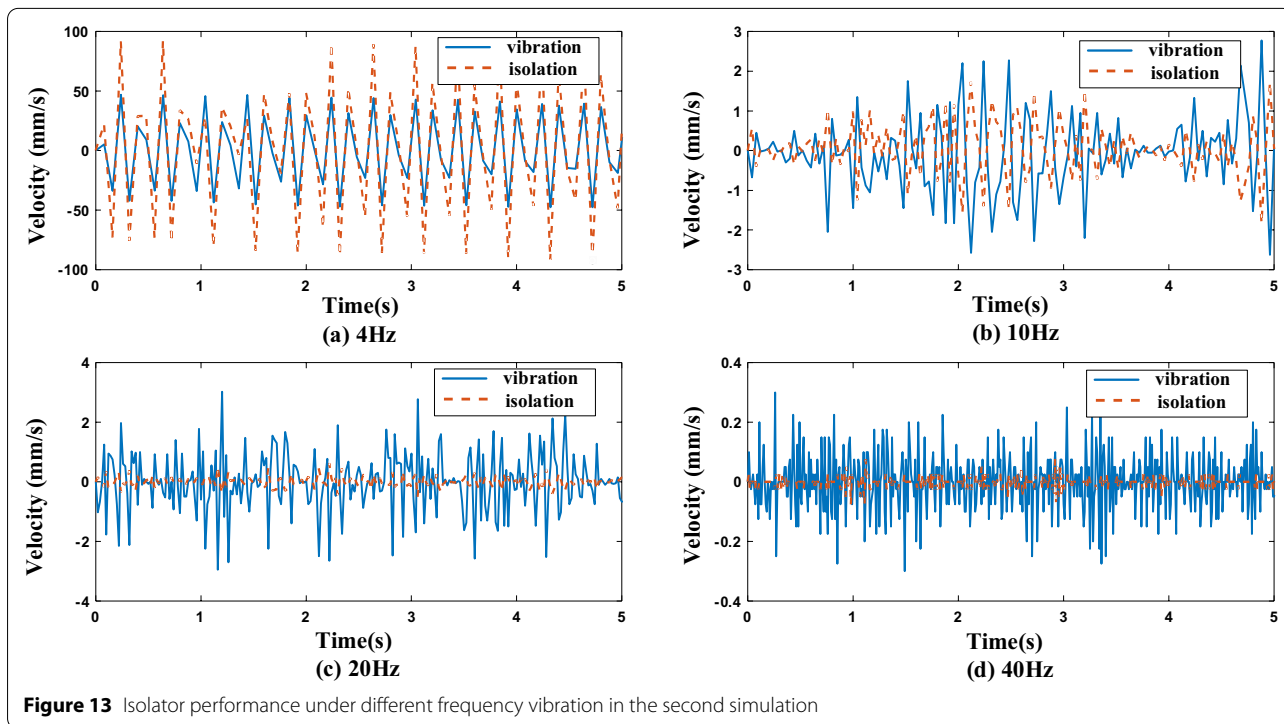
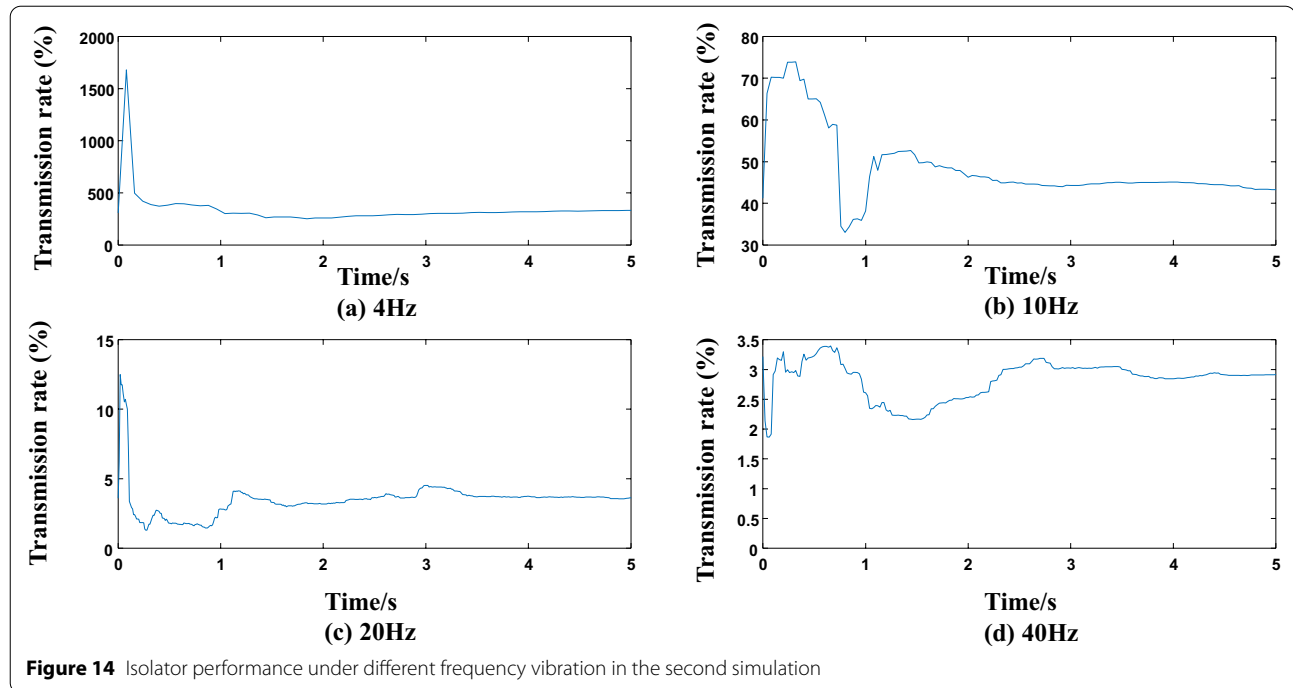


Figure 13 Isolator performance under different frequency vibration in the second simulation



**Figure 14** Isolator performance under different frequency vibration in the second simulation

- (2) Simulation is established in the Matlab/Simulink environment. Through the analysis of the simulation, the pressure control performance is improved with the pressure regulator. Mean vibration velocity and transmission rate decrease under 4, 10, 20 and 40 Hz vibration. But the system with pressure regulator could not achieve the effect of the low frequency vibration isolation such as 4 Hz vibration.
- (3) A multi-frequency band testing system with different payloads is designed and established to detect the performance of the pressure regulator. A comparison between the simulation and the experiment is obtained. The experimental results agree with the simulation results. The error might be caused by the damping of the linear bearing.

For future research, this structure can be converted into an active pneumatic spring for low frequency vibration isolation. If so, this would become an important basis for improving precision manufacturing under low frequency vibration and a fundamental theory for the precise control of pneumatic springs.

#### Acknowledgements

Not applicable.

#### Author contributions

YS designed the whole work. SX was a major contributor in writing the manuscript, ZS analyzed and interpreted the experiment data, and also contributed to the writing of the manuscript. YN contributed to the creation of the experimental platform used in the work and assisted with sampling and laboratory

analyses. YW was in charge of the whole trial and substantively revised it. All authors read and approved the final manuscript.

#### Authors' Information

Yan Shi, born in 1981, is currently a professor at *Beihang University, China*. He received his Ph.D. degree in Mechanical Engineering from *Beihang University, China*, in 2012. His research interests include fluid power transmission system and intelligent robotics. Tel: +86-010-82315821.

Shaofeng Xu, born in 1989, is currently a Ph.D. candidate at *Beihang University, China*. He received his master degree in Mechanical Engineering from *Northwestern Polytechnical University, China*, in 2016.

Zhibo Sun, born in 1988, is currently a lecturer at *Beihang University, China*. He received his Ph.D. degree in Mechanical Engineering from *Beijing Forestry University, China*, in 2016. His research interests focus on mechanism of machinery.

Yulong Nie, born in 1992, is currently a Ph.D. candidate at *Beihang University, China*. He received his master degree in Mechanical Engineering from *Shandong University, China*, in 2019.

Yixuan Wang, born in 1989, is currently a lecturer at *Beihang University, China*. He received his Ph.D. degree in Mechanical Engineering from *Beihang University, China*, in 2019. His research interests focus on fluid power transmission and control.

#### Funding

Supported by National Key Research and Development Project (Grant No. 2021YFC0122502), Youth Fund of National Natural Science Foundation of China (Grant Nos. 52105044, 52105046).

#### Availability of Data and Materials

The datasets used and/or analysed during the current study are available from the corresponding author on reasonable request.

#### Competing Interests

The authors declare no competing financial interests.

#### Author Details

<sup>1</sup>School of Automation Science and Electrical Engineering, Beihang University, Beijing 100191, China. <sup>2</sup>School of Mechanical Engineering, Inner Mongolia

University of Science and Technology, Baotou 014010, China. <sup>3</sup>Engineering Training Center, Beihang University, Beijing 100191, China.

Received: 26 March 2022 Revised: 20 June 2022 Accepted: 2 September 2022

Published online: 22 October 2022

## References

- [1] S H Mirtalebi, A Ebrahimi-Mamaghani, M T Ahmadian. Vibration control and manufacturing of intelligibly designed axially functionally graded cantilevered macro/micro-tubes. *IFAC-PapersOnLine*, 2019, 52(10): 382-387.
- [2] T Zhao, H Chen. Design and experimental study on vibration isolation system of vector sensor application platform. *2019 13th Symposium on Piezoelectricity, Acoustic Waves and Device Applications (SPAWDA)*, Harbin, China, January 11-14, 2019: 1-4.
- [3] L Du, L Ji, Y Luo, et al. Simulation and experiment of an active-passive isolator for micro-vibration control of spacecraft. *2020 15th Symposium on Piezoelectricity, Acoustic Waves and Device Applications (SPAWDA)*, Zhengzhou, China, April 16-19, 2021: 227-232.
- [4] M Zhang, S Luo, C Gao, et al. Research on the mechanism of a newly developed levitation frame with mid-set air spring. *Vehicle System Dynamics*, 2018, 56(12): 1797-1816.
- [5] Z Yang, Z Du, Z Xu, et al. Research on dynamic behavior of train dynamic model of straddle-type monorail. *Noise & Vibration Worldwide*, 2020, 51(11): 195-207.
- [6] Z Zhu, R Wang, L Yang, et al. Modelling and control of a semi-active dual-chamber hydro-pneumatic inerter-based suspension system. *Proceedings of the Institution of Mechanical Engineers, Part D: Journal of Automobile Engineering*, 2021, 235(9): 2355-2370.
- [7] G Gubanov. Broadband pneumatic mass damper for the elimination of workpiece vibrations. *CIRP Journal of Manufacturing Science and Technology*, 2020, 30: 184-194.
- [8] N Y P Vo, T D Le. Static analysis of low frequency isolation model using pneumatic cylinder with auxiliary chamber. *International Journal of Precision Engineering and Manufacturing*, 2020, 21(4): 681-697.
- [9] G Mikułowski. Vibration isolation concept by switchable stiffness on a semi-active pneumatic actuator. *Smart Materials and Structures*, 2021, 30(7): 075019.
- [10] E Palomares, A J Nieto, A L Morales, et al. Numerical and experimental analysis of a vibration isolator equipped with a negative stiffness system. *Journal of Sound and Vibration*, 2018, 414: 31-42.
- [11] Y Nakamura, Y Noguchi, S Wakui. Repetitive control-based vibration attenuation for pneumatic vibration isolators using a phase-lag type compensator. *2019 IEEE International Conference on Mechatronics (ICM)*. Ilmenau, Germany, March 18-20, 2019, 1: 85-90.
- [12] Y M Al-Rawashdeh, M Al-Tamimi, M Heertjes, et al. Micro-positioning end-stage for precise multi-axis motion control in optical lithography machines: preliminary results. *2021 American Control Conference (ACC)*, New Orleans, USA, May 25-28, 2021: 40-47.
- [13] N Oda, S Nishimura. Vibration of air suspension bogies and their design. *Bulletin of JSME*, 1970, 13(55): 43-50.
- [14] J J Chen, Z H Yin, X J Yuan, et al. A refined stiffness model of rolling lobe air spring with structural parameters and the stiffness characteristics of rubber bellows. *Measurement*, 2021, 169: 108355.
- [15] I Mendi-Garcia, N Gil-Negrete Laborda, A Pradera-Mallabiarrena, et al. A survey on the modelling of air springs-secondary suspension in railway vehicles. *Vehicle System Dynamics*, 2022, 60(3): 835-864.
- [16] M Berg. A three-dimensional airspring model with friction and orifice damping. *Vehicle System Dynamics*, 1999, 33(Suppl.1): 528-539.
- [17] H J Zhu, J Yang, Y Q Zhang. Dual-chamber pneumatically interconnected suspension: Modeling and theoretical analysis. *Mechanical Systems and Signal Processing*, 2021, 147: 107125.
- [18] P Pintado, C Ramiro, A L Morales, et al. The dynamic behavior of pneumatic vibration isolators. *Journal of Vibration and Control*, 2018, 24(19): 4563-4574.
- [19] Y H Shin, S J Moon, Y J Kim, et al. Vibration control of scanning electron microscopes with experimental approaches for performance enhancement. *Sensors*, 2020, 20(8): 2277.
- [20] J W Liang, H Y Chen, L C Zeng. Performance enhancement of pneumatic vibration isolators using self-tuning PID feedback and time-delay-control (TDC)-based feedforward scheme. *Proceedings of the ASME 2018 International Design Engineering Technical Conferences and Computers and Information in Engineering Conference*, Quebec City, Canada, August 26-29, 2018, 51852: V008T10A051.
- [21] Y H Shin, K J Kim. Performance enhancement of pneumatic vibration isolation tables in low frequency range by time delay control. *Journal of Sound and Vibration*, 2009, 321(3-5): 537-553.
- [22] T Kato, K Kawashima, K Sawamoto, et al. Active control of a pneumatic isolation table using model following control and a pressure differentiator. *Precision Engineering*, 2007, 31(3): 269-275.
- [23] C Hóš, C Bazsó, A Champneys. Model reduction of a direct spring-loaded pressure relief valve with upstream pipe. *IMA Journal of Applied Mathematics*, 2015, 80(4): 1009-1024.
- [24] S L Prescott, B Ulanicki. Dynamic modeling of pressure reducing valves. *Journal of Hydraulic Engineering*, 2003, 129(10): 804-812.
- [25] T Kato, K Kawashima, T Funaki, et al. A new, high precision, quick response pressure regulator for active control of pneumatic vibration isolation tables. *Precision Engineering*, 2010, 34(1): 43-48.
- [26] X S Wang, Y H Cheng, G Z Peng. Modeling and self-tuning pressure regulator design for pneumatic-pressure-load systems. *Control Engineering Practice*, 2007, 15(9): 1161-1168.
- [27] N Wang, L Y Xu, F Xie, et al. Research on the dynamic characteristics of pneumatic proportional regulator in pneumatic-loading system and design of fuzzy adaptive controller. *Science China Technological Sciences*, 2022: 1-10.
- [28] Y Hao. *Research on Air Spring of Low-Frequency and High-Load*. Nanjing: Nanjing University of Aeronautics and Astronautics, 2007. (in Chinese).
- [29] R Lewandowski, B Chorążyczewski. Identification of the parameters of the Kelvin-Voigt and the Maxwell fractional models, used to modeling of viscoelastic dampers. *Computers & Structures*, 2010, 88(1-2): 1-17.
- [30] P K Wong, Z Xie, J Zhao, et al. Analysis of automotive rolling lobe air spring under alternative factors with finite element model. *Journal of Mechanical Science and Technology*, 2014, 28(12): 5069-5081.
- [31] F W Ning, Y Shi, Y S Cai, et al. Research and application progress of data mining technology in electric power system. *Journal of Advanced Manufacturing Science and Technology*, 2021, 1(3): 1-10.
- [32] B Zhuang, H Xing. Application of nonlinear isolators and define of transmissibility. *J. Mech. Strength*, 1991, 13: 14-17.
- [33] Z B Sun, Y Shi, N Wang, et al. Mechanism and optimization of a novel automobile pneumatic suspension based on dynamic analysis. *Electronics*, 2021, 10(18): 2232.
- [34] Z B Sun, S F Xu, L Cheng, et al. Design and analysis of a pneumatic spring testing system for precision manufacturing. *Materials*, 2022, 15(3): 1121.

Submit your manuscript to a SpringerOpen® journal and benefit from:

- Convenient online submission
- Rigorous peer review
- Open access: articles freely available online
- High visibility within the field
- Retaining the copyright to your article

Submit your next manuscript at ► [springeropen.com](https://www.springeropen.com)